Comparison Results of Medical Image Segmentation with Genetic Algorithm and Particle Swarm Optimization

Maulidya Ikterina and Dwi Ertiningsih

ABSTRACT—Digital-based medical images play an important role in modern health services. Image processing in the form of segmentation imposed on medical images is carried out in order to obtain clear boundaries on images based on certain characteristics. This is expected to reduce errors in further image analysis. In terms of the number of threshold values, the multilevel thresholding method will be applied in this research instead of the bi-level one. To find out the threshold value, the genetic algorithm (GA) and the particle swarm optimization (PSO) algorithm are implemented. These two metaheuristic methods maximize efficiently the form of Shannon, Renyi, and Masi entropies. Furthermore, the threshold value will be applied in the segmentation process of medical images taken from a hospital in Central Java, known as RSUD Kraton Pekalongan. The results of this segmentation are compared by using some image quality indices, including PSNR (Peak Signal to Noise Ratio) and SSIM (Structural Similarity Index Measure) to figure out the most effective method-entropy combination.

***Index Terms*—image segmentation, genetic algorithm, particle swarm optimization, entropy.**

I. INTRODUCTION

DIGITAL image is a projection of a three-dimensional object onto a two-dimensional projection plane [5]. A digital image can be represented through a matrix whose entries correspond with the image's pixels. Pixels are the elements in a digital image at a specific location and contain certain information. A digital image can be subjected to mathematical operations to get the expected new image, this process is called image processing. Image segmentation is a technique in image processing with the aim to separate the image for further analysis based on certain criteria [8]. Digital image processing has been widely used in security, astronomy, medicine, and many application domains [9]. For medical purposes, image segmentation aims to improve image accuracy to make it easier to interpret and minimize disease analysis errors. To illustrate this case, for a cancer patient, medical image segmentation can be applied to identify certain parts of the organ that are too risky to be exposed to high radiation doses, so that the radiotherapy process can be carried out correctly.

There are many different kinds of image segmentation methods. Those are categorized into three main classes: region-based segmentation, edge-based segmentation, and thresholding [9]. This research focuses on thresholding image segmentation. The basic concept of image segmentation using the thresholding method is to divide the pixels on the basis of the intensity level or gray level of an image [5], or simply this method separates the image based on the light and dark differences. Based on the number of threshold values, the thresholding method is classified into bi-level and multilevel thresholding. Bi-level thresholding separates the image into two classes. Meanwhile, multilevel thresholding separates the image into at least three classes. Each class consists of image intensities in an interval separated by predetermined threshold values [4]. The following is an example of a representation equation from the multilevel thresholding method. Given a piecewise function

$$g(x,y)=\begin{cases}0, & \text{if} \quad f(x,y)<T_1\\ 1, & \text{if} \quad T_1\le f(x,y)<T_2\\ 0, & \text{if} \quad T_2\le f(x,y),\end{cases}$$

where,

$f(x,y) =$ grayscale intensity at coordinate(x,y)
$g(x,y) =$ color intensity in binary scale at coordinates(x,y)
$T_1 = 1^{st}$ threshold value
$T_2 = 2^{nd}$ threshold value.

Basically, the optimum threshold value used in image segmentation can be searched by trying all possible threshold values, then selecting the one combination of threshold values that causes the most perfect image segmentation. However, the computational time to find these threshold values grows exponentially according to the number of thresholds given. Therefore, to efficiently determine the required threshold values, the two metaheuristic algorithms, namely the genetic algorithm and particle swarm optimization algorithm will be used.

A. Optimization Method

1) Genetic Algorithm: The genetic algorithm (GA) is one of the many nature-inspired search algorithms. The working principle of genetic algorithms is adapted from the concept of evolution. It continuously updates the individuals in every population to get the better version of them to suit the environmental conditions [3]. In general, the working mechanism of the genetic algorithm is presented in Figure 1. The main operators of the genetic algorithm are selection, crossover, and mutation. These operators are working on

Manuscript received November 23, 2022; revised January, 2024.
This research was funded by Universitas Gadjah Mada through the Final Assignment Recognition (Rekognisi Tugas Akhir) 2021 program.
Maulidya Ikterina is an undergraduate student of the Mathematics Department, Faculty of Mathematics and Natural Sciences, Universitas Gadjah Mada, Yogyakarta, Indonesia (e-mail: maulidyaikterina@mail.ugm.ac.id).
Dwi Ertiningsih is a lecturer in the Mathematics Department, Faculty of Mathematics and Natural Sciences, Universitas Gadjah Mada, Yogyakarta, Indonesia (corresponding author, phone: +62 274552243; e-mail: dwi_ertiningsih@ugm.ac.id).

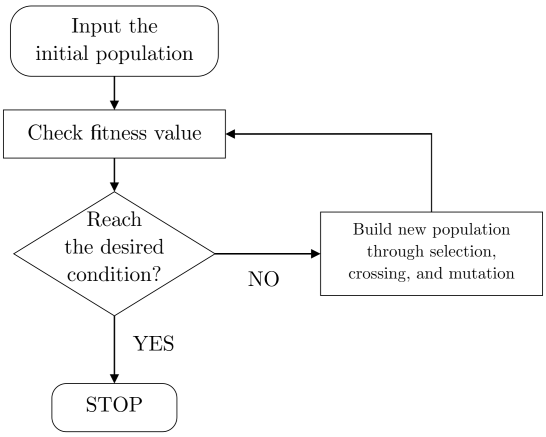

Fig. 1: Genetic Algorithm Flowchart

updating the population process. The step-by-step algorithm is given as follows:

1) Set the number of iterations.
2) Define the fitness function. The fitness function in our study will be the entropy function. Set the population size or the number of individuals in one population, and choose the mutation rate (0 to 1) which will be used as a criterion.
3) Generate the initial population randomly.
4) Evaluate the fitness value of each individual in the population.
5) Repeat the following steps:
   a) Select the two individuals with the best fitness value to become the parents.
   b) Cross the parental chromosomes by selecting chromosomes with certain criteria or just randomly.
   c) Generate the random number (0 to 1) that represents every selected individual's chromosome given. Mutate the chromosome at a rate that is less than the given mutation rate. Here are obtained two new individuals to be included in the next population.
6) Replace the two old individuals with the pre-created offspring. Determination of individuals to be replaced with the offspring is done by selecting individuals with the smallest fitness value.
7) Go to step (5) until the number of iterations is reached.

This algorithm is widely used in optimization problems because it can solve both continuous and discrete optimization problems [9]. The use of many points in the search space simultaneously allows the optimization process to minimize the risk of the results converging only to the local optimal points.

2) Particle Swarm Optimization Algorithm: The particle swarm optimization (PSO) algorithm is another metaheuristics optimization method that is used in this research. This algorithm is also inspired by nature, especially inspired by the behavior of a flock of birds and a group of fish looking for their food location. In the PSO framework, the individuals are referred to as particles and the population is the swarm. Each particle scatters around the search space and adjusts its position based on the experience of the particle itself and other particles around it [12].

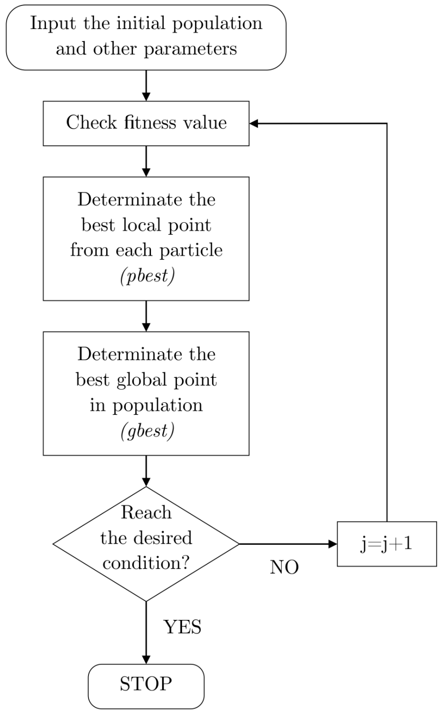

Fig. 2: Particle Swarm Optimization Flowchart

In this algorithm, every i^{th} particle in the j^{th} iteration has its own position and velocity coordinates, both of which affect each other. The position of i^{th} particle in the j^{th} iteration is denoted by x_i^j; $i \in (1, 2, ..., N)$, where N represents the number of particles in the population. While its velocity is expressed as v_i^j.

$$\begin{aligned} x_i^{j+1} &= x_i^j + v_i^{j+1} \\ v_i^{j+1} &= \omega v_i^j + c_1 r_1 (p_{best_i}^j - x_i^j) + c_2 r_2 (g_{best}^j - x_i^j). \end{aligned} \tag{1}$$

It can be seen in Equation (1), parameters c_1 and c_2 respectively represent *learning factor* which indicates the ability of particles and *swarm* in remembering the previous position, while r represents a random number in the interval $[0, 1]$. Based on PSO convergence analysis in [10], the value of $\omega, c_1, \text{and} c_2$ are set with $0 < \omega \leq 1$ and $0 < c_1 + c_2 \leq 4$ to keep the PSO convergent. The best positions of individual and *swarm* in j iteration are denoted as f_{best}^j and g_{best}^j, respectively. In general, the PSO algorithm is shown in Figure 2.

B. Entropy

In information theory, entropy is defined as the average level of uncertainty of an event. The level of information itself is formulated as [14]

$$I(j) = \ln(\frac{1}{P_j}), \tag{2}$$

where $I(j)$ represents the amount of information contained in the event j and P_j represents the probability of an event j. It is clear that if the probability of an event tends to 0, then the value of the information tends to ∞ bits. Meanwhile, consider another event in which probability reaches 1, then the information value will be 0 bits.

Furthermore, entropy is the average of the information values of several events. Shannon [14] formulates the entropy of several events as follows:

$$S(A) = \sum_{j=1}^{N} P_j \ln(\frac{1}{P_j}). \tag{3}$$

It is clear that the higher the entropy value, the more uncertainty in it. On the other hand, the lower the entropy value, the less uncertainty about the event. The entropy formulated by Shannon is known as Shannon entropy. In the image segmentation framework, the information system will be measured by the-gray level intensity distribution of the image. The aim is to maximize the fitness function provided by the entropy functions. Equation (3) can be extended for $k+1$ subsystems, it yields

$$\begin{aligned} S(A_1 + A_2 + ... + A_{k+1}) &= \sum_{i=1}^{k+1} S(A_i) \\ &= \sum_{i=1}^{k+1} \sum_{j=1}^{N} P_{ij} \ln(\frac{1}{P_{ij}}). \end{aligned} \tag{4}$$

1) Renyi Entropy: Renyi entropy was first defined by Renyi as a generalization of Shannon's entropy. Renyi generalizes Shannon's entropy formula and obtains an entropy with parameter α. Renyi entropy is defined [7]

$$R_\alpha(A) = \frac{1}{1-\alpha} \ln \sum_{j=1}^{N} P_j^\alpha, \qquad \alpha \neq 1. \tag{5}$$

As α tends to 1, then we have the following result

$$\lim_{\alpha \to 1} R_\alpha(A) = \sum_{j=1}^{N} P_j ln(\frac{1}{P_j}). \tag{6}$$

Renyi entropy is identical to Shannon entropy when α is tent to 1. In other words, Shannon entropy is a special occurrence of Renyi entropy.

Furthermore, given a system A that consists of $k+1$ independent subsystems $A_1, A_2, \ldots, A_{k+1}$. Then, the total Renyi entropy of the system is defined as

$$\begin{aligned} R_\alpha(A_1 + A_2 + ... + A_{k+1}) &= \sum_{i=1}^{k+1} \frac{1}{1-\alpha} \left[\ln \sum_{j=1}^{N} P_{ij}^\alpha \right], \ \alpha \neq 1 \\ &= \frac{1}{1-\alpha} \sum_{i=1}^{k+1} \ln \sum_{j=1}^{N} P_{ij}^\alpha, \ \alpha \neq 1. \end{aligned} \tag{7}$$

2) Masi Entropy: Masi entropy was first introduced by Masi, which is a combination of Renyi entropy and other entropy called Tsallis entropy [9]. Similar to the Renyi entropy, the Masi entropy is also affected by a parameter r as follows

$$M_r(A) = \frac{1}{1-r} ln \left[1 - (1-r) \sum_{i=1}^{N} P_i \ln P_i \right]. \tag{8}$$

In addition, Masi entropy also satisfies the additivity postulate for systems with $k+1$ subsystems, i.e.

$$\begin{aligned} &M_r(A_1 + A_2 + ... + A_{k+1}) = \\ &\frac{1}{1-r} \sum_{i=1}^{k+1} \ln \left[1 - (1-r) \sum_{j=1}^{N} P_{ij} \ln P_{ij} \right], \quad r \neq 1. \end{aligned}$$

C. Problem Statement

Given a digital image composed of J gray level, with $0 \leq J \leq 255$. Also given $S = \{s_1, s_2, ..., s_J\}$ ordered set containing all the gray levels of the image. Then, from the previously mentioned image, the F matrix can be formed which represents the distribution of the gray level intensities in the image. For every entry of the matrix F, suppose $f(m,n)$ is corresponding to the pixel located at the corresponding position (m,n). The image multilevel thresholding assignment is generally based on the gray level distribution in the matrix F.

The optimum threshold value $t^* \in \{1, 2, ..., J\}$ will be obtained by optimizing the fitness function. Multilevel thresholding in this study has the role of looking for more than one threshold, if it amounts to $k : t_1 < t_2 < ...t_k$ so that the image is divided into $k+1$ classes. Each of the $A_1, ..., A_{k+1}$ subsystems can be expressed as

$$A_1 = \left\{ \frac{P_{s_1}}{\Omega_1}, \frac{P_{s_2}}{\Omega_1}, ..., \frac{P_{s_{t_1}}}{\Omega_1} \right\}, \ \Omega_1 = \sum_{i=1}^{t_1} P_{s_i},$$

$$A_2 = \left\{ \frac{P_{s_{t_1+1}}}{\Omega_2}, \frac{P_{s_{t_1+2}}}{\Omega_2}, ..., \frac{P_{s_{t_2}}}{\Omega_2} \right\}, \ \Omega_2 = \sum_{i=t_1+1}^{t_2} P_{s_i}$$

$$of\vdots$$

$$A_{k+1} = \left\{ \frac{P_{s_{t_k+1}}}{\Omega_{k+1}}, \frac{P_{s_{t_k+2}}}{\Omega_{k+1}}, ..., \frac{P_{s_J}}{\Omega_3} \right\}, \ \Omega_{k+1} = \sum_{i=t_k+1}^{J} P_{s_i},$$

P_{s_i} represents the probability pixel value i appears in the image.

The purpose of multilevel thresholding is to find the best k threshold value $T^* = (t_1^* < \ldots < t_k^*)$ that separate the system A become $A_1, ..., A_{k+1}$ that maximize the total entropy. Threshold values obtained through the two optimizers are then evaluated using image quality indicators. Further, the Shannon, Renyi, and Masi entropies are given as follows, respectively.

$$T_S^* = Argmax \sum_{i=1}^{k+1} S(A_i) \tag{9}$$

$$T_R^* = Argmax \sum_{i=1}^{k+1} R_\alpha(A_i) \tag{10}$$

$$T_M^* = Argmax \sum_{i=1}^{k+1} M_r(A_i). \tag{11}$$

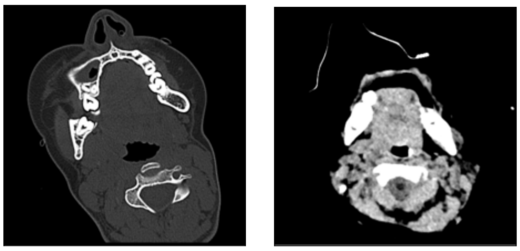

(a) Image 1 (b) Image 2

Fig. 3: Sample Image of The CT Head/Orbita/Colly/Tiroid

D. Image Quality Measurement

1) Peak Signal to Noise Ratio: Peak Signal to Noise Ratio (PSNR) is used to calculate the ratio between the maximum signal power, in terms of the maximum possible gray level intensity, and the power of the distorting noise which affects the quality of its representation [13]. PSNR is one of the most commonly used image quality indexes to measure the quality of lost image compression reconstruction. The signal is considered to be the original data and the noise is the error generated by compression or distortion. The PSNR is represented as

$$PSNR(x,y) = 20\,log_{10}\left(\frac{225}{\sqrt{MSE(x,y)}}\right),$$

where MSE represents the mean of the squared error of the image segmentation output, where the error is the difference between the original image and the segmented one. In Equation (12), the original image and the segmented image are denoted as x and y, respectively. MSE is formulated as follows.

$$MSE(x,y) = \frac{1}{MN}\sum_{i=1}^{M}\sum_{j=1}^{N}(x(i,j) - y(i,j))^2. \tag{12}$$

Note that $M \times N$ represents the resolution or size of the processed image.

2) Structural Index Similarity: Structural Index Similarity (SSIM) is given as [17]

$$SSIM(x,y) = \frac{(2\mu_x\mu_y + C_1)(2\sigma_{xy} + C_2)}{(\mu_{x^2} + \mu_{y^2} + C_1)(\sigma_{x^2} + \sigma_{y^2} + C_2)}, \tag{13}$$

where x and y designates the original and segmented images, μ_x is the mean function, σ_x^2 is the variance function, and σ_{xy} is the covariance between them. The details of the mean, variance, and covariance are given below, respectively.

$$\mu_x = \frac{1}{MN}\sum_{i=1}^{M}\sum_{j=1}^{N}(x(i,j)) \tag{14}$$

$$\sigma_x^2 = \frac{1}{MN-1}\sum_{i=1}^{M}\sum_{j=1}^{N}(x(i,j) - y(i,j))^2 \tag{15}$$

$$\sigma_{xy} = \frac{1}{MN - the1}\sum_{i=1}^{M}\sum_{j=1}^{N}(x(i,j) - \mu_x)(y(i,j) - \mu_y). \tag{16}$$

TABLE I: Mean Values of The PSNR and SSIM of The Sample Images

k	Opt	Entropy	PSNR	SSIM	PSNR's mean	SSIM's mean
2	GA	SE	17.4801	0.5937	17.5090	0.5940
		RE	17.9675	0.6121		
		ME	17.0794	0.5762		
	PSO	SE	17.1017	0.5894	17.4034	0.5916
		RE	17.7435	0.6011		
		ME	17.3650	0.5844		
4	GA	SE	19.9924	0.6838	21.3144	0.7070
		RE	22.8740	0.7281		
		ME	21.0768	0.7091		
	PSO	SE	19.0887	0.6479	21.1982	0.7027
		RE	23.6622	0.7511		
		ME	20.8437	0.7091		
6	GA	SE	24.6695	0.7780	24.4777	0.7717
		RE	25.2091	0.7828		
		ME	23.5546	0.7542		
	PSO	SE	21.2352	0.7316	22.1179	0.7229
		RE	23.2880	0.7306		
		ME	21.8306	0.7066		
10	GA	SE	29.4372	0.8239	28.5109	0.8198
		RE	29.7343	0.8342		
		ME	26.3612	0.8013		
	PSO	SE	27.8676	0.8222	27.6641	0.8174
		RE	27.3805	0.8007		
		ME	27.7443	0.8293		

II. MAIN RESULTS

This section analyzes two medical images (CT Head/Orbita/Colly/Tiroid) from RSUD Kraton, as shown in Figure 3. Those images have been subjected to 6 methods obtained from the combination of two optimizers and three entropies. The experiments are carried out using Python, with the values of $k = 2, 4, 6, 10$, whereas the maximal number of generations is 500 and the population size is fixed to 50 for each optimizer. The parameter r of the ME is 0.1, whereas the parameter α of the Renyi entropy is 0.01. In this study, the color intensity of each region obtained from the segmentation results follows the following rules

$$g(x,y) = \begin{cases} 0, & \text{if } g(x,y) \le T_1 \\ (T_1+1) & \\ \text{ on a scale of } 0 \text{ to } 1, & \text{if } T_1 < g(x,y) \le T_2 \\ \vdots & \\ (T_k+1) & \\ \text{ on a scale of } 0 \text{ to } 1, & \text{if } T_k < g(x,y) \end{cases}$$

where,

$g(x,y) =$ color intensity in binary scale at coordinates(x,y)

$T_1 = 1^{st}$ threshold value on a scale of 1 to 256

$T_k = k^{th}$ threshold value on a scale of 1 to 256.

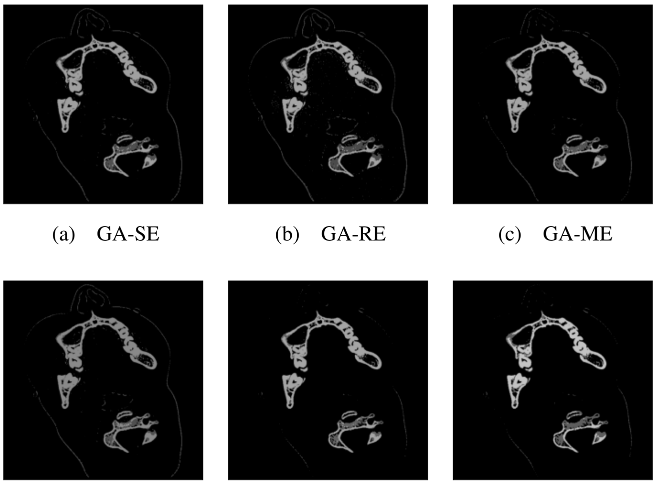

(a) GA-SE (b) GA-RE (c) GA-ME

(d) PSO-SE (e) PSO-RE (f) PSO-ME

Fig. 4: Result of Image 1 for $k = 2$

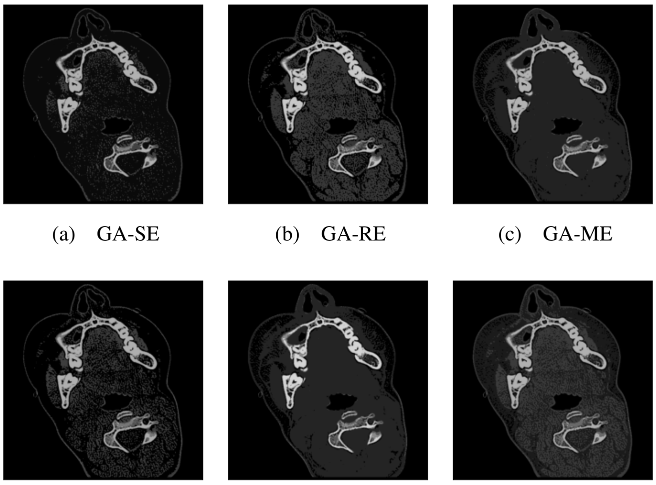

(a) GA-SE (b) GA-RE (c) GA-ME

(d) PSO-SE (e) PSO-RE (f) PSO-ME

Fig. 5: Result of Image 1 for $k = 4$

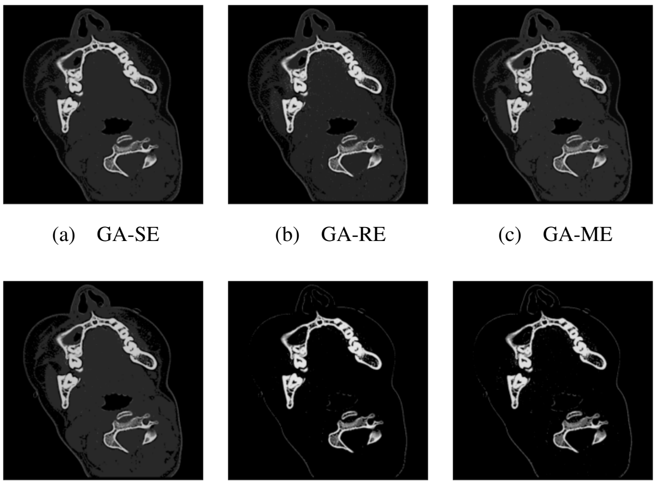

(a) GA-SE (b) GA-RE (c) GA-ME

(d) PSO-SE (e) PSO-RE (f) PSO-ME

Fig. 6: Result of Image 1 for $k = 6$

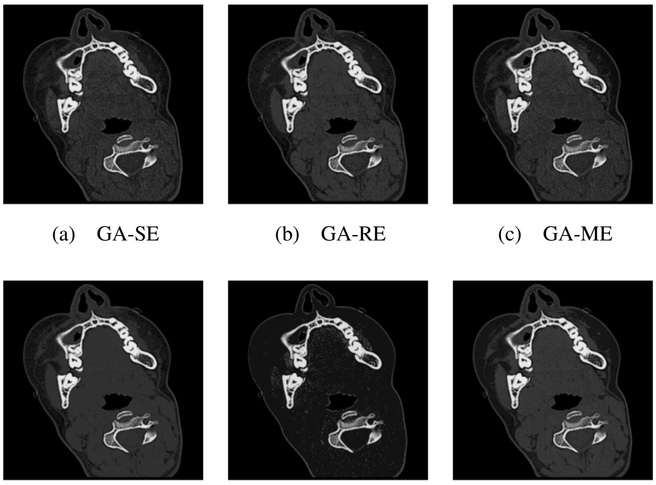

(a) GA-SE (b) GA-RE (c) GA-ME

(d) PSO-SE (e) PSO-RE (f) PSO-ME

Fig. 7: Result of Image 1 for $k = 10$

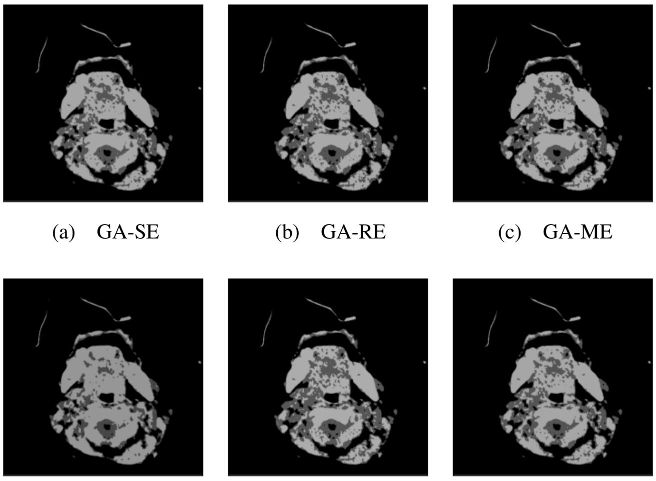

(a) GA-SE (b) GA-RE (c) GA-ME

(d) PSO-SE (e) PSO-RE (f) PSO-ME

Fig. 8: Result of Image 2 for $k = 2$

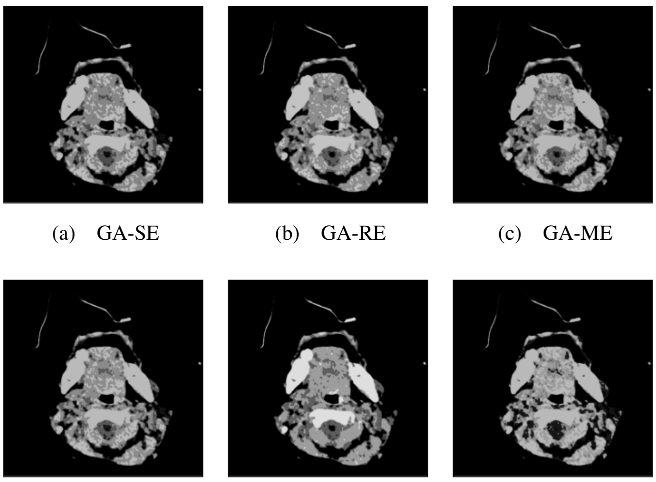

(a) GA-SE (b) GA-RE (c) GA-ME

(d) PSO-SE (e) PSO-RE (f) PSO-ME

Fig. 9: Result of Image 2 for $k = 4$

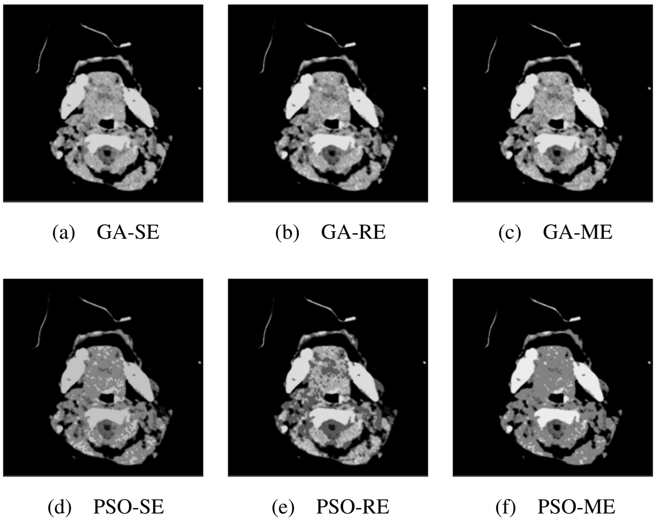

(a) GA-SE (b) GA-RE (c) GA-ME

(d) PSO-SE (e) PSO-RE (f) PSO-ME

Fig. 10: Result of Image 2 for $k = 6$

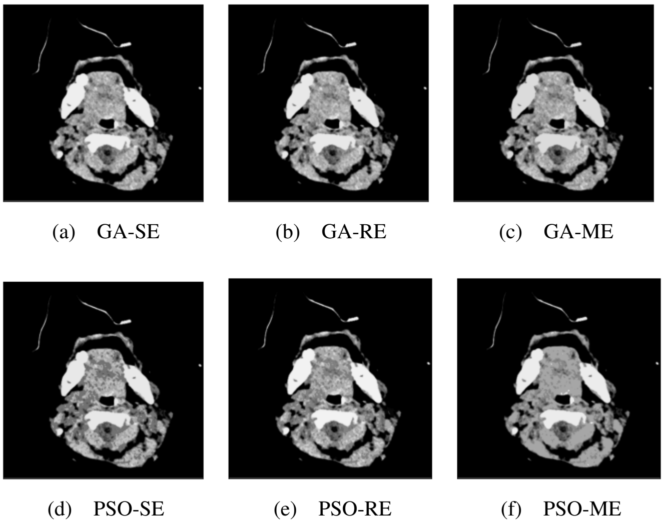

(a) GA-SE (b) GA-RE (c) GA-ME

(d) PSO-SE (e) PSO-RE (f) PSO-ME

Fig. 11: Result of Image 2 for $k = 10$

The Python source code of this research could be accessed at bit.ly/pythonsourcecode. The results obtained as shown in Figures 4 to 10. Table I shows the mean values of the PSNR and SSIM indices on sample images achieved by the six optimizer-entropy combinations for some values of thresholds k, $k = 2, 4, 6, 10$, respectively. From the Table I, we have comparative performances of the two optimizers, i.e. GA and PSO, combined with 3 entropies SE, RE, and ME, as follows:

(i) In general, higher k value is result in higher PSNR and SSIM values. In other words, the more threshold values are applied, the better image segmentation is obtained.
(ii) Overall, the optimization methods using Renyi entropy result in a better segmentation than the other two entropies.
(iii) The genetic algorithm generates better threshold values to apply in the whole segmentations than the PSO does.

III. CONCLUDING REMARKS

This research discusses six methods of combination optimizer-entropy to obtain the optimum threshold value used in the multilevel thresholding segmentation process applied to two medical images taken from RSUD Kraton, Pekalongan. The two optimizers, i.e. GA and PSO, were applied to maximize the value of the entropy as a fitness function, combining with Renyi, Masi, and Shannon entropies. The segmentation results have been evaluated with metrics PSNR and SSIM indexes for comparison purposes.

The numerical experiments yield several interesting conclusions. Generally, it's concluded that GA's performance is better than PSO's since the PSNR and SSIM values of the GA are more dominant than PSO. It shows that the Renyi entropy is more suitable for performing multilevel thresholding in medical image processing. Additionally, we have shown that maximizing entropy does not necessarily lead to the maximization of evaluation metrics such as PSNR and SSIM. Future investigations could broaden the comparative analysis by incorporating different entropy measures and optimization algorithms, while also considering diverse image types.

ACKNOWLEDGMENT

We gratefully acknowledge Ari Dwi Reskianto from the RSUD Kraton, Pekalongan, for assistance and two sample images of CT Head/Orbita/Colly/Tiroid provided.

REFERENCES

[1] D. A. Coley, *An Introduction to Genetic Algorithms for Scientists and Engineers*. Singapore: World Scientific Publishing Co. Pte. Ltd., Singapore, 1999.
[2] H. Anton, *Elementary Linear Algebra*, 8th ed.New York: John Wiley and Sons, Inc., 2000.
[3] M. Gen and R. Cheng, *Genetic Algorithms and Engineering Design*.Canada: John Wiley dan Sons, Inc., 1996.
[4] R. C. Gonzalez and R. E. Woods, *Digital Image Processing*, 4th ed.New York: Pearson, 2018.
[5] V. Tyagi, *Understanding Digital Image Processing*.Boca Raton: Taylor and Francis Group, 2018.
[6] Y. Arkeman, K. B. Seminar, and H. Gunawan, *Algoritma Genetika. Teori dan Aplikasinya untuk Bisnis dan Industri*.Bogor: IPB Press, 2012.
[7] J. C. Baez, "Renyi Entropy and Free Energy," *Quantum Physics*, vol. 3, no.1102.2098, pp. 1-5, 2011.
[8] P. A. Cahyan, M. Aswin, A. Mustofa, "Segmentasi Citra Digital dengan Menggunakan Algoritma Watershed dan Lowpass Filter sebagai Proses Awal," *Jurnal Mahasiswa TEUB*, vol. 1, no.1, pp. 1-6, 2013.
[9] I. H. Jaghdam, A. B. Ishak, S. A. Khalek, and A. Jamal, "Quantum and Classical Genetic Algorithms for Multilevel Segmentation of Medical Images: A Comparative Study," *Computer Communications*, vol. 162, pp. 83-93, 2020.
[10] Y. Hongtao, L. Wenguang, and L. Zhenqiang, "Convergence Analysis of Particle Swarm Optimizer and Its Improved Algorithm Based on Velocity Differential Evolution," *Computational Intelligence and Neuroscience*, vol. 2013, 2013.
[11] P. Mohammadi, A. Ebrahimi-Moghadam, S. Shirani, "Subjective and Objective Quality Assessment of Image: A Survey," *Majlesi Journal of Electrical Engineering*, vol. 9, no.1, 2015. rah D. S. Rahayu, C. Fatichah, and R. Sulaiman, "Peningkatan Efisiensi Waktu Komputasi dengan Metode Pemrograman Dinamis," *Jurnal Simantec*, vol. 3, no.3, pp. 122-131, 2013.
[12] A. Rosita, Y. Purwanto, and R. Soelaiman, "Implementasi Algoritma Particle Swarm untuk Menyelesaikan Sistem Persamaan Nonlinear," *Jurnal Teknik ITS*, vol. 1, pp. 211-215, 2012.
[13] U. Sara, M. Akter, and M. S. Uddin, "Image Quality Assessment through FSIM, SSIM, MSE and PSNR—A Comparative Study," *Journal of Computer and Communications*, vol. 7, pp. 8-18, 2019.
[14] C. E. Shannon, "A mathematical Theory of Communication," *Bell System Technical Journal*, vol. 27, no.3, pp. 379–423, 1948.
[15] R. R. Sharapov and A. V. Lapshin, "Convergence of Genetic Algorithm,Pattern Recognition and Image Analysis," *Mathematical Theory of Pattern Recognition* vol.16, pp.392-397, 2006.
[16] W. Shu, "A Quantum Genetic Simulated Annealing Algorithm for Task Scheduling," *Advances in Computation and Intelligence*, vol. 4683, pp. 169-176, 2007.

[17] Z. Wang, dkk., vImage Quality Assessment: From Error Visibility to Structural Similarity," *IEEE Transactions on Image Processing*, vol. 13, no. 4, 2004.

[18] J. Kennedy and R. Eberhart, "Particle Swarm Optimization," in *Proceedings of ICNN'95 - International Conference on Neural Networks 1995*, Perth.